

Polynuclear Complexes of Macrocyclic Oxamide with Thiocyanate: Syntheses, Crystal Structures and Magnetic Properties

Ya-Qiu Sun,^{*,[a,b]} Dong-Zhao Gao^[a] Wen Dong^[c] Dai-Zheng Liao,^{*,[d]} and Chen-Xi Zhang^[e]

Keywords: Organic–inorganic hybrid composites / Magnetic properties / Heterometallic complexes / Bridging ligands / Macrocyclic ligands

Five complexes with the formula $\{[(\text{CuL})_2\text{Cr}(\mu\text{-SCN})_2]\text{OH}\}_n$ (**1**), $[\text{Mn}(\text{CuL})_2(\text{NCS})_2]$ (**2**), $[\text{Cu}(\text{CuL})_2(\text{NCS})_2]$ (**3**), $[\text{Ni}(\text{CuL})_2(\text{NCS})_2]$ (**4**) and $[\text{Co}(\text{CuL})(\text{NCS})_2(\text{CH}_3\text{OH})_2]_2$ (**5**), ($\text{H}_2\text{L} = 2, 3\text{-dioxo-5,6,14,15-dibenzo-1,4,8,12-tetraazacyclopentadeca-7,13-diene}$) were synthesized and structurally determined. The structure of **1** has oxamido-bridged trinuclear $[\text{Cr}^{\text{III}}\text{Cu}^{\text{II}}_2]$ units and consists of a 1D helical chain formed by the linking of copper(II) and chromium(III) ions through the oxamido and $\mu_{1,3}$ -NCS bridges. The structure of **2**, **3** or **4** consists of oxamido-bridged trinuclear $[\text{M}^{\text{III}}\text{Cu}^{\text{II}}_2]$ molecules (for **2–4**, $\text{M} =$

Mn, Cu, Ni, respectively) and arranges in a 1D zig-zag chain. Complex **5** is a composed of a tetranuclear $[\text{Co}^{\text{II}}\text{Cu}^{\text{II}}_2]$ molecule with both the oxamido and $\mu_{1,3}$ -NCS bridges. The variable-temperature magnetic susceptibility measurements (2–300 K) of **1**, **2**, **4** and **5** show pronounced antiferromagnetic interactions between the copper(II) atom and neighbouring metal ions.

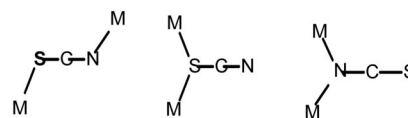
(© Wiley-VCH Verlag GmbH & Co. KGaA, 69451 Weinheim, Germany, 2009)

Introduction

Polynuclear complexes are of considerable interest for the design of new magnetic materials and the investigation of the structure and role of polymetallic active sites in biological systems.^[1] Among the polynuclear complexes, heterospin complexes have received particular attention. Magnetic interaction between two nonequivalent paramagnetic centres may lead to a situation that cannot be encountered with species containing only one kind of centre, but heterospin complexes can provide various and unexpected structural topologies.^[2] From the magnetic viewpoint, the magnetic interaction between nearest nonequivalent neighbouring spin carriers may be ferromagnetic; it may also be antiferromagnetic with noncompensation of the local spins. In the latter case, the most favourable situation is that the dif-

ference between the nonequivalent local spins is as large as possible. The synthesis and magnetic properties of manganese(II)–copper(II) complexes with $S_{\text{Mn}} = 5/2$ and $S_{\text{Cu}} = 1/2$ local spins is an active area of research. The first molecular-based heterobimetallic magnets were found to be the oxamato- and oxamido-bridged manganese(II)–copper(II) species.^[3]

On the other hand, the synthesis of homo- and heterometallic transition-metal complexes supported by the pseudohalide NCO ,^[4] NCS ,^[5] NCSe ,^[6] N_3 ,^[7] and $\text{N}(\text{CN})_2$ ^[8] bridges has attracted special attention in view of the architectural diversity and interesting magnetic properties of the complexes obtained. In this context, the thiocyanato ligand presents ambidentate ability with an end-on ($\mu_{\text{N,N}}$ -NCS and $\mu_{\text{S,S}}$ -SCN) or an end-to-end ($\mu_{\text{N,S}}$ -NCS) coordination mode (Scheme 1).^[5]



Scheme 1. Different bridging modes of the thiocyanato ion.

However, despite the various modes of coordination of the NCS group to the metal ions and despite its ability to act as an efficient mediator for the magnetic interaction between the paramagnetic ions centres, it is not widely used for the design and synthesis of complexes that simultaneously have thiocyanato ligand bridges and other ligand

[a] Tianjin Key Laboratory of Structure and Performance for Functional Molecule, College of Chemistry and Life Science, Tianjin Normal University, Tianjin 300387, P. R. China
E-mail: syq@nankai.edu.cn

[b] Tianjin Key Laboratory of Cyto-Genetical and Molecular Regulation, College of Chemistry and Life Science, Tianjin Normal University, Tianjin 300387, P. R. China
E-mail: hxsyq@mail.tjnu.edu.cn

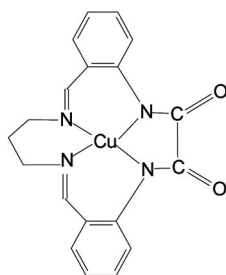
[c] Department of Chemistry, Guangzhou University, Guangzhou 510006, P. R. China
E-mail: dw320@yahoo.com.cn

[d] Department of Chemistry, Nankai University, Tianjin 300071, P. R. China
E-mail: liaodz@nankai.edu.cn

[e] Tianjin University Science and Technology, School of Science, Tianjin, P. R. China

bridges.^[9] To obtain this type of desired system, planar tetraazo macrocyclic ligands were used. Cyclam and its substituted derivatives are the most widespread tetraazo macrocyclic ligands.^[10,11] Francese et al. were the first to use the simple macrocyclic copper(II) complex $\text{Cu}(\text{cyclam})^{2+}$ in order to obtain a heterometallic system $\{[\text{Cu}(\text{cyclam})][\text{Co}(\text{NCS})_4]\}_n$.^[10] Compared with tetraazo macrocyclic complexes of Cu^{II} and Ni^{II} , macrocyclic oxamido complexes of Cu^{II} and Ni^{II} cannot only provide two free coordination places at the metal atom, but also contain potential donors for another metal ion.^[3,12–16] However, thiocyanato-bridged complexes with macrocyclic oxamido ligands are rare.^[9b,9d]

With these facts in mind and in continuation of our interest in homo- and heterometallic polynuclear complexes, by using the thiocyanato ligand and the prepared macrocyclic oxamido complex ligand (Scheme 2), we synthesized and characterized the compounds $\{[(\text{CuL})_2\text{Cr}(\mu\text{-SCN})_2]\text{OH}\}_n$ (**1**), $[\text{Mn}(\text{CuL})_2(\text{NCS})_2]$ (**2**), $[\text{Cu}(\text{CuL})_2(\text{NCS})_2]$ (**3**), $[\text{Ni}(\text{CuL})_2(\text{NCS})_2]$ (**4**) and $[\text{Co}(\text{CuL})(\text{NCS})_2(\text{CH}_3\text{OH})_2]$ (**5**), and studied the magnetic properties of **1**, **2**, **4** and **5**.



Scheme 2. The macrocyclic oxamido complex ligand CuL.

Results and Discussion

Synthesis and Formulation

By using thiocyanato and macrocyclic oxamido mixed ligands as the metal linker, five new complexes were synthesized by a slow diffusion method. The molar ratio of the starting materials, reagent molar ratios and the reaction temperature play an important role in the formation of these five compounds. Complex **1** was obtained at 35 °C, complexes **2–4** were obtained at 18 °C, and compound **5** was obtained at 25 °C. The differences in reagent molar ratios and temperature leads to differences in solubility and diffusibility of the starting materials, which results in different structures of the five compounds.

Description of the Structure

The structure unit of **1** consists of a trinuclear $[(\text{CuL})_2\text{Cr}(\mu\text{-SCN})_2]^+$ moiety and a monovalent anion OH^- ; a perspective view of it is depicted in Figure 1, and selected bond lengths and angles are listed in Table 1.

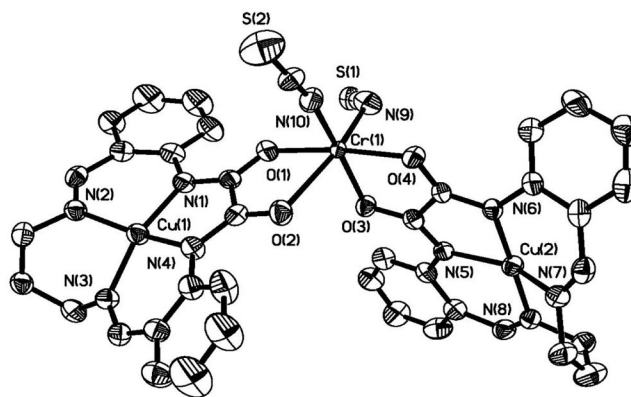


Figure 1. Perspective view of the trinuclear cation $[(\text{CuL})_2\text{Cr}(\mu\text{-SCN})_2]^+$ of **1**.

Table 1. Selected bond lengths [Å] and angles [°] for **1**.^[a]

Cr1–N10	1.965(7)	O3–Cr1–N9	87.3(2)
Cr1–O4	1.990(4)	N10–Cr1–O2	88.6(2)
Cr1–O1	2.011(5)	O4–Cr1–O2	103.56(18)
Cr1–O3	2.028(4)	O1–Cr1–O2	73.44(18)
Cr1–N9	2.263(7)	O3–Cr1–O2	83.36(18)
Cr1–O2	2.395(5)	N9–Cr1–O2	157.3(2)
Cu1–N2	1.914(6)	N2–Cu1–N4	161.7(3)
Cu1–N4	1.919(5)	N2–Cu1–N3	91.4(3)
Cu1–N3	1.938(6)	N4–Cu1–N3	93.6(2)
Cu1–N1	1.942(5)	N2–Cu1–N1	94.6(2)
Cu2–N6	1.933(5)	N4–Cu1–N1	87.3(2)
Cu2–N8	1.939(6)	N3–Cu1–N1	158.0(2)
Cu2–N7	1.991(6)	N6–Cu2–N8	178.6(2)
Cu2–N5	1.992(5)	N6–Cu2–N7	89.8(2)
Cu2–S1#1	2.736(2)	N8–Cu2–N7	91.6(2)
N10–Cr1–O4	93.1(2)	N6–Cu2–N5	84.5(2)
N10–Cr1–O1	93.6(2)	N8–Cu2–N5	94.0(2)
O4–Cr1–O1	172.59(19)	N7–Cu2–N5	152.0(2)
N10–Cr1–O3	168.7(2)	N6–Cu2–S1#1	87.10(15)
O4–Cr1–O3	81.07(17)	N8–Cu2–S1#1	93.16(17)
O1–Cr1–O3	91.80(18)	N7–Cu2–S1#1	95.67(17)
N10–Cr1–N9	103.0(3)	N5–Cu2–S1#1	111.39(15)
O4–Cr1–N9	95.3(2)	C39–S1–Cu2#2	99.2(3)
O1–Cr1–N9	86.3(2)	C1–O1–Cr1	122.7(5)

[a] Symmetry transformations used to generate equivalent atoms: #1: $-x + 1/2, y - 1/2, -z + 1/2$; #2: $-x + 1/2, y + 1/2, -z + 1/2$.

In the $[(\text{CuL})_2\text{Cr}(\mu\text{-SCN})_2]^+$ unit, the central chromium(III) ion is linked to two external copper(II) ions through the *exo-cis* oxygen donors of the macrocyclic oxamido ligand and two thiocyanato ligands in a *cis* configuration. The chromium(III) ion has a distorted octahedral geometry with four oxygen atoms from two oxamido bridges and two nitrogen atoms from two thiocyanato ligands. The Cr–N distances vary from 1.965(7) to 2.263(7) Å, and Cr–O distances from 1.990(4) to 2.395(5) Å. The external Cu^{2+} ion is coordinated to four nitrogen atoms from the macrocyclic ligand, and the $[\text{CuN}_4]$ chromophore plane is distorted from planarity. The deviation of the four nitrogen atoms from their mean plane are 0.3469, -0.3211 , 0.3370 and -0.3374 Å, respectively, and the copper ion is -0.0254 Å out of the plane. The $[(\text{CuL})_2\text{Cr}(\mu\text{-SCN})_2]^+$ units

are alternately bridged by a thiocyanato group in an end-to-end mode to form a 1D helical chain in which the Cu–S bond length is 2.736(2) Å (Figure 2).

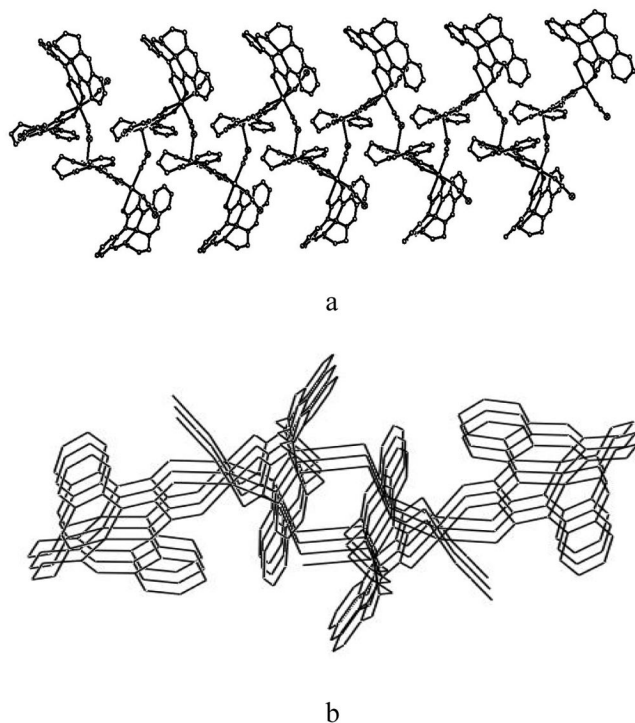


Figure 2. Schematic representation of the asymmetric oxamido-bridged trinuclear unit of **1** generating a 1D helical chain through $\mu_{1,3}$ -NCS bridges.

Compounds **2–4** are isostructural, hence only the structure of **2** will be discussed in detail. For **2–4**, selected bond lengths and angles are listed in Tables 2, 3, and 4. A perspective view of the structure of the trinuclear $\text{Mn}(\text{CuL})_2(\text{SCN})_2$ unit is depicted in Figure 3. The structure of **2** consists of trinuclear $\text{Mn}(\text{CuL})_2(\text{SCN})_2$ molecules in which the central manganese(II) ion is located on a twofold axis and linked to two $[\text{CuL}]$ complex ligands and two thiocyanato ligands in a *cis* configuration. The copper(II) ion resides in a slightly distorted square planar environment with two amidate nitrogen atoms and two imino nitrogen atoms from the macrocyclic oxamido ligand as donors. The manganese(II) ion has a *cis* octahedral geometry with four oxygen atoms from two oxamido bridges [the Mn–O distances is 2.171(3)–2.299(3) Å] and two nitrogen atoms from two thiocyanato ligands [the Mn–N distances is 2.130(4)–2.178(4) Å]. The central manganese(II) ion is linked to each external copper(II) ion through *exo-cis* oxygen donors of the macrocyclic oxamido ligand. The three metal ions form a V-type arrangement through the bridges, with a Cu...Mn separation of 5.4959 Å and a Cu...Cu separation of 8.4162 Å. As depicted in Figure 4, the $[(\text{CuL})_2\text{MnSCN}_2]$ units are alternately bridged by a thiocyanato group in an end-to-end mode to form a 1D zig-zag chain in which the Cu–S bond length is 3.147 Å, and the Cu–S distance is dis-

tinctly longer than most reported values (2.33–2.95 Å);^[5] however, it still lies in the typical range (2.2–3.2 Å) observed for Cu–SCN bonds in coordination compounds.^[5e,5h]

Table 2. Selected bond lengths [Å] and angles [°] for **2**.

Cu1–N8	1.936(3)	Cu1–N6	1.938(3)
Cu1–N5	1.947(3)	Cu1–N7	1.956(3)
Cu2–N4	1.962(4)	Cu2–N2	1.970(3)
Cu2–N1	1.978(3)	Cu2–N3	1.993(3)
Mn3–N9	2.130(4)	Mn3–O1	2.171(3)
Mn3–N10	2.178(4)	Mn3–O3	2.191(3)
Mn3–O4	2.238(3)	Mn3–O2	2.299(3)
N8–Cu1–N6	159.60(14)	N8–Cu1–N5	86.49(13)
N6–Cu1–N5	94.66(13)	N8–Cu1–N7	93.40(14)
N6–Cu1–N7	90.99(14)	N5–Cu1–N7	164.01(13)
N4–Cu2–N2	173.08(16)	N4–Cu2–N1	89.94(16)
N2–Cu2–N1	83.13(13)	N4–Cu2–N3	95.19(16)
N2–Cu2–N3	91.68(13)	N1–Cu2–N3	171.42(14)
N9–Mn3–O1	111.01(14)	N9–Mn3–N10	89.86(15)
O1–Mn3–N10	94.57(12)	N9–Mn3–O3	93.08(13)
O1–Mn3–O3	150.21(10)	N10–Mn3–O3	103.03(12)
N9–Mn3–O4	165.84(13)	O1–Mn3–O4	82.40(10)
N10–Mn3–O4	93.68(13)	O3–Mn3–O4	72.76(10)
N9–Mn3–O2	93.40(14)	O1–Mn3–O2	72.59(10)
N10–Mn3–O2	167.08(12)	O3–Mn3–O2	89.29(10)
O4–Mn3–O2	86.19(10)	O1–C1–N1	127.8(4)

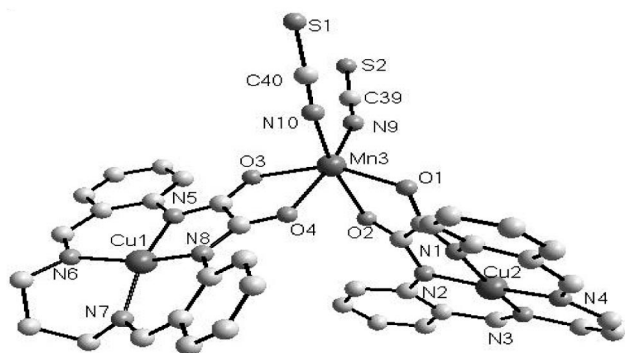
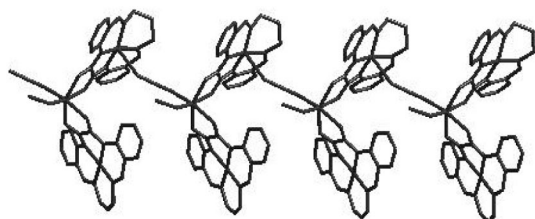
Table 3. Selected bond lengths [Å] and angles [°] for **3**.

Cu1–N3	1.933(8)	Cu1–N1	1.937(8)
Cu1–N4	1.945(8)	Cu1–N2	1.947(7)
Cu2–N8	1.964(9)	Cu2–N7	1.975(8)
Cu2–N6	1.985(7)	Cu2–N5	1.990(7)
Cu3–N9	2.109(10)	Cu3–N10	2.166(9)
Cu3–O3	2.171(6)	Cu3–O2	2.199(7)
Cu3–O1	2.244(7)	Cu3–O4	2.286(6)
N3–Cu1–N1	159.9(3)	N3–Cu1–N4	91.2(4)
N1–Cu1–N4	93.5(4)	N3–Cu1–N2	93.9(3)
N1–Cu1–N2	86.8(3)	N4–Cu1–N2	164.3(3)
N8–Cu2–N7	94.4(4)	N8–Cu2–N6	174.3(4)
N7–Cu2–N6	91.2(3)	N8–Cu2–N5	91.0(4)
N7–Cu2–N5	171.6(3)	N6–Cu2–N5	83.2(3)
N9–Cu3–N10	89.7(4)	N9–Cu3–O3	112.1(3)
N10–Cu3–O3	94.7(3)	N9–Cu3–O2	92.3(3)
N10–Cu3–O2	102.5(3)	O3–Cu3–O2	150.3(3)
N9–Cu3–O1	165.0(3)	N10–Cu3–O1	93.5(3)
O3–Cu3–O1	82.3(2)	O2–Cu3–O1	72.8(2)
N9–Cu3–O4	93.7(3)	N10–Cu3–O4	167.8(3)
O3–Cu3–O4	73.1(2)	O2–Cu3–O4	89.1(2)
O1–Cu3–O4	86.3(2)	C1–N1–C19	122.6(9)

A perspective view of the tetranuclear $[\text{Co}(\text{CuL})(\text{NCS})_2(\text{CH}_3\text{OH})_2]_2$ complex **5**, which incorporates a macrocyclic oxamido group is depicted in Figure 5, and selected bond lengths and angles are listed in Table 5. The oxamido and μ -SCN groups alternately bridge the Cu^{II} and Co^{II} ions, which results in the formation of a cyclic tetranuclear molecule; the four metal ions are in the same plane. The Co^{II} atom coordinates two oxygen donors of the macrocyclic oxamido ligand, two nitrogen atoms from two NCS^- ions and two oxygen atoms from two CH_3OH groups. The cobalt centres have a distorted octahedral geometry, which can be seen from the N–Co–O bond angles that vary from 169.21(12) to 174.17(11)° and the O–Co–O bond angle of 165.14(11)°. Furthermore, one of the coordinated NCS^-

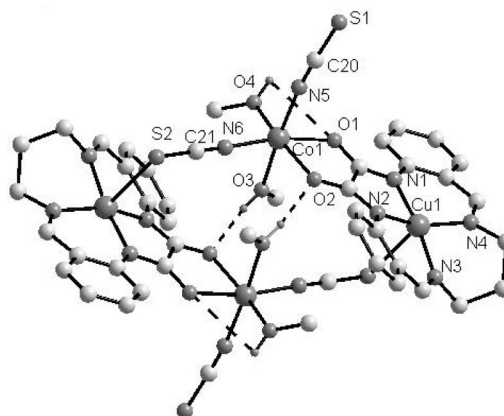
Table 4. Selected bond lengths [Å] and angles [°] for **4**.

Ni1–N1	2.031(4)	Ni1–N2	2.092(3)
Ni1–O4	2.093(2)	Ni1–O1	2.112(2)
Cu1–N4	1.937(3)	Cu1–N6	1.942(3)
Cu1–N3	1.950(3)	Cu1–N5	1.957(3)
Cu2–N9	1.956(8)	Cu2–N7	1.971(3)
Cu2–N8	1.983(3)	Cu2–N10	2.009(3)
Cu2–N9'	2.034(7)	N1–Ni1–N2	91.53(13)
N1–Ni1–O4	107.40(12)	N2–Ni1–O4	94.32(11)
N1–Ni1–O1	92.77(12)	N2–Ni1–O1	101.93(11)
O4–Ni1–O1	153.75(10)	N1–Ni1–O2	168.64(11)
N2–Ni1–O2	92.92(12)	O4–Ni1–O2	82.69(10)
O1–Ni1–O2	76.08(10)	N1–Ni1–O3	91.71(12)
N2–Ni1–O3	169.70(11)	O4–Ni1–O3	75.38(9)
O1–Ni1–O3	87.68(10)	O2–Ni1–O3	85.73(10)
N4–Cu1–N6	159.68(13)	N4–Cu1–N3	86.63(13)
N6–Cu1–N3	94.63(13)	N4–Cu1–N5	92.90(13)
N6–Cu1–N5	91.34(14)	N3–Cu1–N5	164.00(13)
N9–Cu2–N7	168.6(2)	N9–Cu2–N8	93.0(2)
N7–Cu2–N8	82.82(12)	N9–Cu2–N10	93.2(2)
N7–Cu2–N10	92.03(12)	N8–Cu2–N10	171.57(13)
N9–Cu2–N9'	21.1(3)	N7–Cu2–N9'	166.4(3)
N8–Cu2–N9'	87.6(2)	N10–Cu2–N9'	96.3(2)

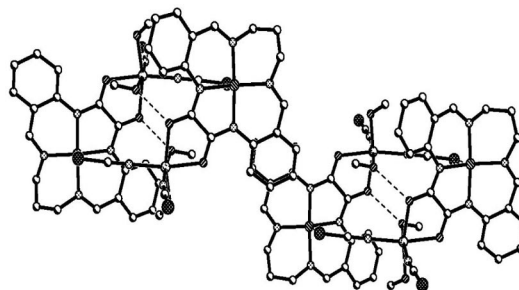
Figure 3. Perspective view of the trinuclear $\text{Mn}(\text{CuL})_2(\text{SCN})_2$ molecules of **2**.Figure 4. Schematic representation of the asymmetric oxamido-bridged trinuclear unit of **2** generating to a 1D zig-zag chain through $\mu_{1,3}$ -NCS bridges.

ions acts as a terminal ligand, and the other one adopts an end-on-end coordination mode that bridges the Co^{II} and Cu^{II} ions. The distance between the Co^{II} and Cu^{II} ions bridged by NCS^- is 6.1406 Å, while that bridged by the oxamido group is 5.3751 Å. The coordination geometry around the Cu^{II} ion is a slightly distorted square pyramid, with a τ value of 0.237 calculated from $\tau = (\beta - \alpha)/60$.^[17] The axial position is occupied by a sulfur atom, and the Cu–S distance is 2.8886 Å. In the $[\text{Co}(\text{CuL})(\text{NCS})_2]$ -

$(\text{CH}_3\text{OH})_2$ framework, there are O–H \cdots O interactions between the coordinated CH_3OH groups and the oxygen atoms of the oxamido groups ($d_{\text{O}\cdots\text{O}} = 2.8114$ Å), which enhance the stability of **5** (Figure 5). In addition, there are π – π interactions between the benzene rings of the CuL moieties of different tetranuclear molecules in the cell that are parallel to each other, and the distance between the carbon atoms is about 3.652 Å. The π – π interactions enable the formation of a 1D supramolecular chain (Figure 6).

Figure 5. Perspective view of the $[\text{Co}(\text{CuL})(\text{NCS})_2(\text{CH}_3\text{OH})_2]_2$ molecules of **5**.Table 5. Selected bond lengths [Å] and angles [°] for **5**.

Cu1–N4	1.947(3)	Cu1–N2	1.954(3)
Cu1–N1	1.962(3)	Cu1–N3	1.970(3)
Co1–N6	2.042(3)	Co1–O4	2.073(3)
Co1–N5	2.075(4)	Co1–O1	2.103(3)
Co1–O2	2.132(3)	Co1–O3	2.173(3)
N4–Cu1–N2	156.90(14)	N4–Cu1–N1	93.99(13)
N2–Cu1–N1	85.65(13)	N4–Cu1–N3	90.46(13)
N2–Cu1–N3	93.53(13)	N1–Cu1–N3	170.50(14)
N6–Co1–O4	97.12(13)	N6–Co1–N5	98.28(13)
O4–Co1–N5	92.89(13)	N6–Co1–O1	169.21(12)
O4–Co1–O1	89.20(11)	N5–Co1–O1	90.09(12)
N6–Co1–O2	95.54(12)	O4–Co1–O2	165.14(11)
N5–Co1–O2	92.95(12)	O1–Co1–O2	77.14(10)
N6–Co1–O3	87.42(13)	O4–Co1–O3	85.16(12)
N5–Co1–O3	174.17(11)	O1–Co1–O3	84.40(11)
O2–Co1–O3	87.67(11)	C1–O1–Co1	115.6(2)

Figure 6. View of the self-assembly, 1D supermolecular architecture through π – π interactions for **5**.

IR and Electronic Spectra

The IR spectra of the five complexes are similar and clearly show the existence of the thiocyanato and macro-

cyclic oxamido moieties in the molecules. The IR spectra of **1–5** show three strong bands around 1639, 1610 and 1448 cm^{-1} , which are characteristic of the bridging oxamido group and can be attributed to the $\nu(\text{N}-\text{C}-\text{O})$ stretching bands.^[13] The bands of almost equal intensity at 2143 and 2076 cm^{-1} are attributed to SCN^- ^[18] and are characteristic of end-to-end bridging and terminal thiocyanato groups, respectively. The solid-state electronic absorption spectra of complexes **1–5** were measured. In the spectra of complexes **1–5**, the broad absorption band at 633 nm can be assigned to the spin-allowed d–d electronic transition for Cu^{II} ($3d^9$) in a C_{4v} symmetry.^[14,19] The electronic absorption spectra of other metal ions were not observed, because the absorption intensity is very weak. All complexes exhibit intense bands below 500 nm, which can be assigned to charge-transfer transitions in the $[\text{CuL}]$ chromophores and/or to intraligand $\pi-\pi^*$ interactions.^[14]

Magnetic Property

The magnetization measurements for complexes **1–4** have been carried out under a magnetic field strength of 2 kOe. The magnetic susceptibility (χ_{M}) and $\chi_{\text{M}}T$ of complex **1** in the temperature range 2–300 K are shown in Figure 7. The $\chi_{\text{M}}T$ value is equal to 2.43 $\text{cm}^3\text{mol}^{-1}\text{K}$ at 300 K, which is lower than that expected if $\text{Cu}^{\text{II}}-\text{Cr}^{\text{III}}-\text{Cu}^{\text{II}}$ trinuclear metal centres have no interactions (2.62 $\text{cm}^3\text{mol}^{-1}\text{K}$). When the complex is cooled, the $\chi_{\text{M}}T$ value progressively decreases in the range from 300 K to 2 K. On the basis of the crystal structure of **1**, there should be three kinds of magnetic interactions for the present system, namely, (i) $\text{Cu}^{\text{I}}\cdots\text{Cr}^{\text{I}}$ through the oxamido bridge in one trinuclear unit, (ii) $\text{Cu}^{\text{II}}\cdots\text{Cr}^{\text{I}}$ through the oxamido bridge in one trinuclear unit, and (iii) $\text{Cu}^{\text{II}}\cdots\text{Cr}^{\text{I}}$ through the thiocyanato bridges between adjacent trinuclear units. To the best of our knowledge, there is no formula in the literature to deal with the magnetic susceptibility of such a complicated system. In order to simplify the experimental results, the linear dependence of the reciprocal magnetic susceptibilities, χ_{M}^{-1} , on temperature gives the Weiss constant ($\theta = -15.97\text{ K}$), which indicates an antiferromagnetic interaction in complex **1**.

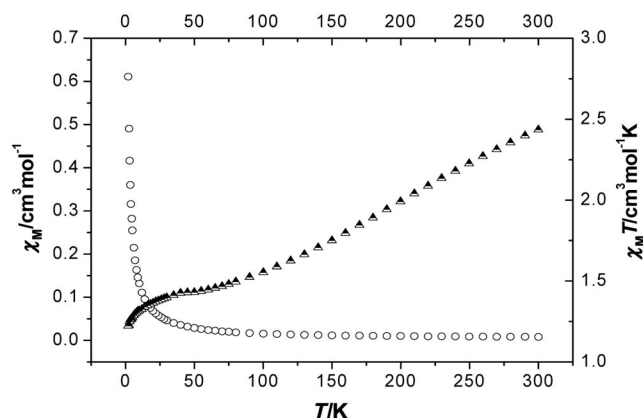


Figure 7. χ_{M} (O) vs. T and $\chi_{\text{M}}T$ (Δ) vs. T plots for complex **1**.

The magnetic susceptibility (χ_{M}) and $\chi_{\text{M}}T$ of complex **2** in the temperature range 2–300 K are shown in Figure 8. The $\chi_{\text{M}}T$ value of **2** at room temperature is 4.75 $\text{cm}^3\text{mol}^{-1}\text{K}$, lower than the spin-only value (4.84 $\text{cm}^3\text{mol}^{-1}\text{K}$) expected for the uncoupled $\text{Cu}^{\text{II}}-\text{Mn}^{\text{II}}-\text{Cu}^{\text{II}}$ trinuclear system ($S_{\text{Cu}} = 1/2$ and $S_{\text{Mn}} = 5/2$). The $\chi_{\text{M}}T$ value decreases smoothly upon cooling and reaches a near plateau value of 2.07 $\text{cm}^3\text{mol}^{-1}\text{K}$ below 16 K. The plateau value is close to the spin-only value for $S_{\text{T}} = 3/2$ (2.00 $\text{cm}^3\text{mol}^{-1}\text{K}$) resulting from the antiferromagnetic spin coupling between Cu^{II} and Mn^{II} ions in the trinuclear system. On the basis of the crystal structure of **2** (Figures 3 and 4), there are two kinds of magnetic interactions for the present system from a magnetic viewpoint, namely, (i) intra-molecular $\text{Cu}^{\text{II}}-\text{Mn}^{\text{II}}-\text{Cu}^{\text{II}}$ interactions through the oxamido bridges and (ii) intermolecular interactions between the adjacent trinuclear molecules through $\mu_{1,3}-\text{NCS}$ coordination interactions. By taking into account the two kinds of interactions, the magnetic analysis was then carried out by using the theoretical expression of the magnetic susceptibility deduced from the spin Hamiltonian $\hat{H} = -2J(\hat{S}_{\text{Cu}}\hat{S}_{\text{Mn}} + \hat{S}_{\text{Cu}}\hat{S}_{\text{Mn}})$. The expression for the magnetic susceptibility was obtained as follows [Equation (1)].

$$\chi_{\text{tri}} = \frac{N\beta^2}{4kT} \frac{A}{B} \quad (1)$$

$$A = 10g_1^2 + 35g_2^2 \exp\left(\frac{5J}{kT}\right) + 35g_{\text{Mn}}^2 \exp\left(\frac{7J}{kT}\right) + 84g_3^2 \exp\left(\frac{12J}{kT}\right)$$

$$B = 2 + 3 \exp\left(\frac{5J}{kT}\right) + 3 \exp\left(\frac{7J}{kT}\right) + 4 \exp\left(\frac{12J}{kT}\right)$$

$$g_1 = (7g_{\text{Mn}} - 2g_{\text{Cu}})/5$$

$$g_2 = (31g_{\text{Mn}} + 4g_{\text{Cu}})/35$$

$$g_3 = (5g_{\text{Mn}} + 2g_{\text{Cu}})/7$$

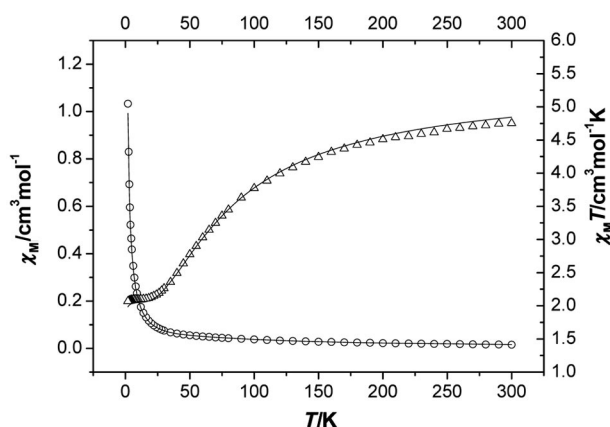


Figure 8. χ_{M} (O) vs. T and $\chi_{\text{M}}T$ (Δ) vs. T plots for complex **2**.

J is the exchange integral between Cu^{II} and Mn^{II} through the oxamido bridge, χ_{tri} is the magnetic susceptibility in the absence of the molecular field, and g_{Mn} and g_{Cu} are the local g factors, assumed to be isotropic. For the magnetic

interactions between the adjacent trinuclear molecular units, the molecular field approximation was used and is illustrated in Equation (2).

$$\chi_M = \chi_{\text{tri}} / [1 - \chi_{\text{tri}}(2zj' / Ng^2\beta^2)] \quad (2)$$

where χ_M is the exchange-coupled magnetic susceptibility actually measured and zj' is the exchange parameter between the trinuclear molecular units. The least-squares fit to the experimental data was found with $J = -13.48 \text{ cm}^{-1}$, $zj' = -0.021 \text{ cm}^{-1}$, $g_{\text{Mn}} = 2.07$, $g_{\text{Cu}} = 2.00$ (fixed), and the agreement factor, defined as $R = \Sigma[(\chi_M)^{\text{calcd}} - (\chi_M)^{\text{obsd}}]^2 / \Sigma[(\chi_M)^{\text{obsd}}]^2$, is 1.13×10^{-3} . The J value suggests a pronounced intramolecular antiferromagnetic interaction between the copper(II) and manganese(II) ions through the oxamido bridges, and the zj' value suggests a very weak intermolecular antiferromagnetic interaction through the $\mu_{1,3}$ -SCN coordination interactions. Comparing with some manganese(II)–copper(II) species that incorporate noncyclic oxamido or macrocyclic oxamido ligands reported previously, the exchange integral in **2** is in the range of those reported.^[9b,9d,14f,14h,16d,16e,20]

The magnetic susceptibility (χ_M) and $\chi_M T$ of complex **4** in the temperature range 2–300 K are shown in Figure 9. The $\chi_M T$ value is $1.51 \text{ cm}^3 \text{ mol}^{-1} \text{ K}$ at 300 K, which is slightly higher than the spin-only value ($1.46 \text{ cm}^3 \text{ mol}^{-1} \text{ K}$) expected for the uncoupled $\text{Cu}^{\text{II}}\text{--Ni}^{\text{II}}\text{--Cu}^{\text{II}}$ trinuclear system ($S_{\text{Cu}} = 1/2$ and $S_{\text{Ni}} = 1$). The $\chi_M T$ value decreases smoothly when cooled and reaches a near plateau value below 16 K, and the $\chi_M T$ value at 3 K is $2.74 \times 10^{-7} \text{ cm}^3 \text{ mol}^{-1} \text{ K}$. The plateau value is close to the spin-only value for $S_T = 0$ ($0.00 \text{ cm}^3 \text{ mol}^{-1} \text{ K}$) resulting from the antiferromagnetic spin coupling between Cu^{II} and Ni^{II} ions in the trinuclear system. On the basis of the isotropic spin Hamiltonian $\hat{H} = -2J(\hat{S}_{\text{Cu}1}\hat{S}_{\text{Ni}} + \hat{S}_{\text{Cu}2}\hat{S}_{\text{Ni}})$, the expression for the magnetic susceptibility for a $\text{Cu}^{\text{II}}\text{--Ni}^{\text{II}}\text{--Cu}^{\text{II}}$ system is as follows [Equation (3)].

$$\chi_{\text{tri}} = \frac{N\beta^2}{2kT} \frac{A}{B} \quad (3)$$

$$A = (g_{\text{Ni}} + g_{\text{Cu}})^2 [5 + \exp(-\frac{4J}{kT})] + 4g_{\text{Ni}}^2 \exp(-\frac{2J}{kT})$$

$$B = 5 + 3\exp(-\frac{4J}{kT}) + \exp(-\frac{6J}{kT}) + 3\exp(-\frac{2J}{kT})$$

J is the exchange integral between Cu^{II} and Ni^{II} through the oxamido bridge. The molecular field approximation was used for magnetic interactions between the adjacent trinuclear molecular units and is illustrated in Equation (2).

The least-squares fit to the experimental data was found with $J = -30.71 \text{ cm}^{-1}$, $zj' = -0.99 \text{ cm}^{-1}$, $g_{\text{Ni}} = 2.04$, $g_{\text{Cu}} = 2.00$ (fixed), and $R = 1.76 \times 10^{-3}$. The J value suggests a pronounced intramolecular antiferromagnetic interaction between the copper(II) and nickel(II) ions through the oxamido bridges, and the zj' value suggests a very weak intermolecular antiferromagnetic interaction through the $\mu_{1,3}$ -SCN coordination interactions. The antiferromagnetic interaction through the oxamido group arises from the non-zero overlap between the magnetic orbitals around Cu^{II} and

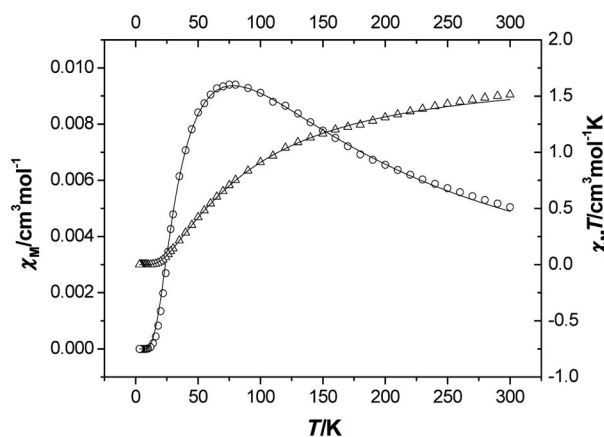


Figure 9. χ_M (O) vs. T and $\chi_M T$ (Δ) vs. T plots for complex **4**.

Ni^{II} ,^[1a] and the J value for **4** is less than those reported in the literature for the Cu--Ni heteronuclear complexes with oxamido bridges.^[20c,20e,21]

The temperature dependence of the magnetic susceptibility of **5** in the range 2–300 K is shown in Figure 10. The $\chi_M T$ value is $2.52 \text{ cm}^3 \text{ mol}^{-1} \text{ K}$ at 300 K, which is larger than the spin-only value ($2.25 \text{ cm}^3 \text{ mol}^{-1} \text{ K}$) expected for the uncoupled $\text{Cu}^{\text{II}}\text{--Co}^{\text{II}}$ binuclear system ($S_{\text{Cu}} = 1/2$ and $S_{\text{Co}} = 3/2$). On lowering the temperature, $\chi_M T$ decreases continuously and reaches $0.16 \text{ cm}^3 \text{ mol}^{-1} \text{ K}$ at 2 K. The shape of the $\chi_M T$ vs. T curve suggests an overall antiferromagnetic behaviour. To the best of our knowledge, no formula to reproduce the magnetic susceptibility of such a complex system is available in the literature; we therefore used an approximate method to interpret the magnetic behaviour. Complex **5** can be regarded as a dimer formed by Cu--Co dinuclear units, which are indicated in Scheme 3, and only first-neighbour interactions were considered. Simultaneously, the contribution of the spin-orbit coupling of the Co^{II} ion is considered according to van Vleck's equation.^[22] On the basis of the spin Hamiltonian $\hat{H} = -2J\hat{S}_{\text{Cu}}\hat{S}_{\text{Co}} + g\beta\hat{H}_Z\hat{S}_Z$, the susceptibility for the dinuclear unit CuCo ,

$$\chi_{\text{CoCu}} = \frac{N\beta^2}{kT} \left[\frac{10g_2^2 + 2g_1^2 \exp(-\frac{4J}{kT})}{5 + 3\exp(-\frac{4J}{kT})} \right] + N_A \quad (4)$$

$$g_2 = \frac{1}{4}g_{\text{Cu}} + \frac{3}{4}g_{\text{Co}}$$

$$g_1 = \frac{-1}{4}g_{\text{Cu}} + \frac{5}{4}g_{\text{Co}}$$

$$g_{\text{Co}} = \sqrt{\frac{3kT\chi_{\text{Co}}}{N\beta^2 S(S+1)}}$$

$$\chi_{\text{Co}} = \frac{N\beta^2}{3kT} \frac{F_1}{F_2}$$

$$F_1 = \frac{7\lambda(3-A)^2}{5kT} + \frac{12(2+A)^2}{25A} + \left[\frac{2\lambda(11-2A)^2}{45kT} + \frac{176(A+2)^2}{675A} \right] \exp(-\frac{5A\lambda}{2kT}) + \left[\frac{\lambda(A+5)^2}{9kT} - \frac{20(A+2)^2}{27A} \right] \exp(-\frac{4A\lambda}{kT})$$

$$F_2 = \frac{\lambda}{3kT} [3 + 2\exp(-\frac{5A\lambda}{2kT}) + \exp(-\frac{4A\lambda}{kT})]$$

$$\chi_M = \chi_{\text{CoCu}} / [1 - \chi_{\text{CoCu}}(2zj' / Ng^2\beta^2)] \quad (5)$$

χ_{CoCu} , is calculated from Equation (4), and the magnetic susceptibility of the tetranuclear complex can be calculated from Equation (5).

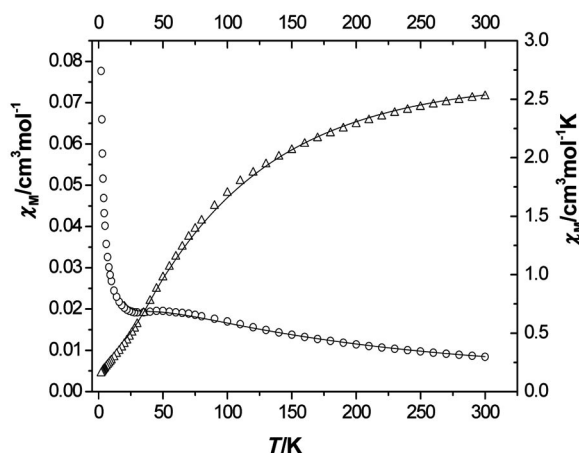
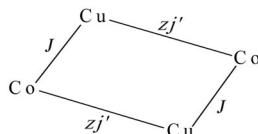


Figure 10. χ_M (O) vs. T and $\chi_M T$ (Δ) vs. T plots for complex **5**.



Scheme 3. The model for the magnetic interaction in **5**.

where J is the exchange integral between Cu^{II} and Co^{II} ions through the oxamido bridge, and zJ' is the intermolecular exchange integral of the Cu–Co dinuclear units. N_a is the temperature-independent paramagnetic term and is set as $326 \times 10^{-6} \text{ m}^3 \text{ mol}^{-1}$. A is ligand field parameter, and λ is spin-orbit coupling parameter. The least-squares fit to the experimental data was found with $J = -15.69 \text{ cm}^{-1}$, $g_{\text{Cu}} = 2.10$ (fixed), $zJ' = -1.17 \text{ cm}^{-1}$, $A = 1.19$, $\lambda = -170 \text{ cm}^{-1}$ (fixed), and $R = 7.40 \times 10^{-4}$. The points below 20 K cannot be reproduced with this model, which may be attributed to the zero-field splitting with the Co^{II} ion of the $S = 1/2$ state. The fitted results show that the oxamido bridge promotes an antiferromagnetic interaction between the Cu^{II} and Co^{II} ions, and the doubly bridged $\mu_{1,3}$ -NCS coordination (the intermolecular exchange integral of Cu–Co dinuclear units) gives rise to a slightly antiferromagnetic interaction. In addition, spin-orbit coupling of the Co^{II} ion plays an important role in the magnetic behaviour.

For complexes **1**, **2**, **4** and **5**, the paramagnetic metal ions bridged by the oxamido moiety present antiferromagnetic coupling between the central and macrocyclic metals. According to Kahn, the antiferromagnetic interaction between Cu^{II} and the central metal ions ($M = \text{Cr}$ **1**; Mn **2**, Ni **4** and Co **5**) arises from the nonzero overlap between the magnetic orbitals centred at the metal ions and delocalized toward the ligands.^[1a] A larger overlap of the magnetic orbitals leads to a stronger interaction.^[1a] The J value of complex **4** is lower than that of complex **2**. The difference may be attributed to the following reasons: (i) the $\text{Cu} \cdots M$ distance is larger for **2** ($\text{Cu} \cdots \text{Mn} = 5.50 \text{ \AA}$) than for **4** ($\text{Cu} \cdots \text{Ni} =$

$5.52\text{--}5.30 \text{ \AA}$) and (ii) the energies of the 3d orbitals of Mn^{II} are higher than the corresponding ones in Ni^{II} . Therefore there is less overlap between the two adjacent magnetic orbitals in **2** than in complex **4**.

Conclusions

The structures and magnetic properties of complexes containing both a thiocyanato-bridge and oxamido-bridge were investigated. The $[(\text{CuL})_2\text{Cr}(\mu\text{-SCN})_2]^+$ units of **1** are alternately bridged by NCS^- in an end-to-end mode to form a 1D helical chain, and antiferromagnetic interactions are exhibited. To the best of our knowledge, the magnetic behaviour of **1** oxamido-bridged $\text{Cu}(\text{II})$ –chromium(III)–copper(II) heterotrimeric complexes have not been reported. Single-crystal X-ray analyses revealed that compounds **2–4** are isostructural. Comparing the magnitude of the interaction in **2** and **4** trinuclear $\text{Cu}^{\text{II}}\text{--}M^{\text{II}}\text{--Cu}^{\text{II}}$ species containing the same ligands but different M^{II} ions, we obtained the following sequence for the magnetic interaction: $\text{Cu}^{\text{II}}\text{--Ni}^{\text{II}}\text{--Cu}^{\text{II}} > \text{Cu}^{\text{II}}\text{--Mn}^{\text{II}}\text{--Cu}^{\text{II}}$, which is in accordance with Kahn's expectation.^[23] In $[\text{Co}(\text{CuL})(\text{NCS})_2(\text{CH}_3\text{OH})_2]_2$, the Cu^{II} and Co^{II} ions are bridged by oxamido and NCS^- ligands. The magnetic behaviours of oxamido-bridge and NCS^- bridge give rise to antiferromagnetic interactions.

Experimental Section

Material and Synthesis: All the starting reagents were of A.R. grade and were used as purchased. The complex ligand CuL was prepared as described elsewhere.^[24] The complex ligand NiL was prepared in the same way as CuL.

$\{[(\text{CuL})_2\text{Cr}(\mu\text{-SCN})_2\text{OH}]_n$ (1**):** Single crystals of **1** were grown in a methanol solution by a slow diffusion method using an H-shaped tube. The precursor CuL (0.2 mmol) and $\text{Cr}(\text{ClO}_4)_3 \cdot 6\text{H}_2\text{O}$ (0.1 mmol) were added in one arm, and NaSCN (0.2 mmol) in the other; methanol (15 mL) was then added in the tube. Brown–green crystals, suitable for X-ray determination, were formed after several days [yield 39.6 mg, 40.5% based on $\text{Cr}(\text{ClO}_4)_3 \cdot 6\text{H}_2\text{O}$]. $\text{C}_{40}\text{H}_{33}\text{CrCu}_2\text{N}_{10}\text{O}_5\text{S}_2$ (976.96): calcd. C 49.13, H 3.37, N 14.33; found C 49.15, H 3.33, N 14.38. IR (KBr): $\tilde{\nu} = 2144$ (vs), 2076 (vs), 1640 (vs), 1608 (vs), 1500 (vs), 1481 (m), 1346 (vs, br.), 1080 (vs, br.), 915 (w), 770 (w) cm^{-1} .

$[\text{M}(\text{CuL})_2(\text{NCS})_2]$ ($M = \text{Mn}$, Cu , Ni) **2–4:** Complexes **2–4** were prepared in the same manner as **1**. The precursor CuL (0.1 mmol) and $\text{Mn}(\text{ClO}_4)_2 \cdot 6\text{H}_2\text{O}$ ($M = \text{Mn}$, Cu , Ni) (0.1 mmol) were added in one arm, and NaSCN (0.2 mmol) in the other; methanol (10 mL) was then added in the tube. Brown–green crystals, suitable for X-ray determination, were formed after several days [yield: for **2**, 35.1 mg, 36.5% based on $\text{Mn}(\text{ClO}_4)_2 \cdot 6\text{H}_2\text{O}$; for **3**, 34.0 mg, 30.5% based on $\text{Cu}(\text{ClO}_4)_2 \cdot 6\text{H}_2\text{O}$; for **4**, 38.2 mg, 39.5% based on $\text{Ni}(\text{ClO}_4)_2 \cdot 6\text{H}_2\text{O}$]. **2**: $\text{C}_{40}\text{H}_{32}\text{Cu}_2\text{MnN}_{10}\text{O}_4\text{S}_2$ (962.94): calcd. C 49.85, H 3.32, N 14.54; found C 49.83, H 3.33, N 14.51. **3**: $\text{C}_{40}\text{H}_{32}\text{Cu}_3\text{N}_{10}\text{O}_4\text{S}_2$ (971.55): calcd. C 49.41, H 3.29, N 14.41; found C 49.35, H 3.33, N 14.48. **4**: $\text{C}_{40}\text{H}_{32}\text{Cu}_2\text{N}_{10}\text{NiO}_4\text{S}_2$ (966.67): calcd. C 49.66, H 3.31, N 14.48; found C 49.65, H 3.33, N 14.45. IR (KBr): $\tilde{\nu} = 2143$ (vs), 2076 (vs), 1640 (vs), 1604 (vs), 1500 (vs), 1481 (m), 1342 (vs, br.), 1080 (vs, br.), 915 (w), 770 (w) cm^{-1} .

Table 6. Crystal data and structure refinement for complexes 1–3.

	1	2	3
Formula	C ₄₀ H ₃₃ CrCu ₂ N ₁₀ O ₅ S ₂	C ₄₀ H ₃₂ CuMn ₂ N ₁₀ OS ₂	C ₄₀ H ₃₂ Cu ₃ N ₁₀ O ₄ S ₂
<i>F</i> _w	976.96	962.94	971.55
Crystal system	monoclinic	monoclinic	monoclinic
Space group	<i>P</i> 2 ₁ / <i>n</i>	<i>C</i> 2/ <i>c</i>	<i>C</i> 2/ <i>c</i>
<i>a</i> [Å]	17.399(5)	13.9265(2)	13.9349(13)
<i>b</i> [Å]	11.180(3)	14.4221(2)	14.4250(13)
<i>c</i> [Å]	23.300(7)	38.3589(6)	38.368(3)
<i>α</i> [°]	90	90	90
<i>β</i> [°]	109.054(4)	92.9610(10)	93.001(5)
<i>γ</i> [°]	90	90	90
<i>V</i> [Å ³]	4284(2)	7694.1(2)	7701.7(12)
<i>Z</i>	4	8	8
<i>ρ</i> _{calcd.} [g cm ^{−3}]	1.515	1.663	1.676
Crystal size [mm]	0.24 × 0.22 × 0.20	0.209 × 0.207 × 0.043	0.209 × 0.203 × 0.053
<i>T</i> [K]	293(2)	293(2)	293(2)
GoF	1.041	1.043	0.998
<i>R</i> ₁ ^[a] [<i>I</i> > 2σ(<i>I</i>)]	0.0639	0.0497	0.0794
<i>wR</i> ₂ ^[b] [<i>I</i> > 2σ(<i>I</i>)]	0.1850	0.1063	0.1991

[a] $R_1 = \Sigma||F_o| - |F_c||/\Sigma|F_o|$. [b] $wR_2 = \{\Sigma[w(F_o^2 - F_c^2)^2]/\Sigma[w(F_o^2)]\}^{1/2}$.

[Co(CuL)(NCS)₂(CH₃OH)₂]₂ (**5**): The complex was prepared by a slow diffusion method using an H-shaped tube. The precursor CuL (0.1 mmol) and Co(ClO₄)₂·6H₂O (0.1 mmol) were added in one arm, and NaSCN (0.2 mmol) in the other; methanol (13 mL) was then added in the tube. Brown–green crystals, suitable for X-ray determination, were formed after several days [yield 27.6 mg, 43.5% based on Co(ClO₄)₂·6H₂O]. C₂₃H₂₄CoCuN₆O₄S₂ (635.07): calcd. C 43.46, H 3.78, N 13.23; found C 43.45, H 3.73, N 13.28. IR (KBr): $\tilde{\nu}$ = 2140 (vs), 2076 (vs), 1641 (vs), 1600 (vs), 1500 (vs), 14861 (m), 1348 (vs, br.), 1079 (vs, br.), 915 (w), 770 (w) cm^{−1}.

Caution! Perchlorate salts of metal complexes with organic ligands are potentially explosive and should be handled in small quantities with care.

Physical Measurements: Analyses of C, H and N were determined on a Perkin–Elmer 240 Elemental analyzer. IR spectra were recorded as KBr discs on a Shimadzu IR-408 infrared spectropho-

tometer in the 4000–600 cm^{−1} range. Electronic spectra for solid samples were recorded on a Shimadzu UV-2101 PC scanning spectrophotometer. Variable-temperature magnetic susceptibilities were measured on an MPMS-7 SQUID magnetometer. Diamagnetic corrections were made with Pascal's constants for all the constituent atoms.^[25]

X-ray Crystallography: The data were collected on a Bruker Smart-1000-CCD area detector by using graphite-monochromated Mo-*K*_α radiation (λ = 0.71073 Å). The structures were solved by direct methods and subsequent Fourier difference techniques and refined by using the full-matrix least-squares procedure on *F*² with anisotropic thermal parameters for all non-hydrogen atoms (SHELXS-97 and SHELXL-97).^[26] Hydrogen atoms were added geometrically and refined with riding model position parameters and fixed isotropic thermal parameters. Crystal data collection and refinement parameters are given in Tables 6 and 7. CCDC-709746, -709747, -709748, -709749 and -709750 contain the supplementary crystallographic data for this paper. These data can be obtained free of charge from The Cambridge Crystallographic Data Centre via www.ccdc.cam.ac.uk/data_request/cif.

Table 7. Crystal data and structure refinement for complexes 4 and 5.

	4	5
Formula	C ₄₀ H ₃₂ Cu N ₁₀ Ni ₂ O ₄ S ₂	C ₂₃ H ₂₄ CoCuN ₆ O ₄ S ₂
<i>F</i> _w	966.67	635.07
Crystal system	monoclinic	monoclinic
Space group	<i>C</i> 2/ <i>c</i>	<i>P</i> 2 ₁ / <i>c</i>
<i>a</i> [Å]	13.785(3)	12.991(3)
<i>b</i> [Å]	14.351(3)	21.786(4)
<i>c</i> [Å]	38.148(8)	9.1815(18)
<i>α</i> [°]	90	90
<i>β</i> [°]	93.16(3)	101.83(3)
<i>γ</i> [°]	90	90
<i>V</i> [Å ³]	7535(3)	2543.5(9)
<i>Z</i>	8	4
<i>ρ</i> _{calcd.} [g cm ^{−3}]	1.704	1.658
Crystal size [mm]	0.22 × 0.20 × 0.12	0.10 × 0.08 × 0.04
<i>T</i> [K]	293(2)	113(2)
GoF	1.031	1.102
<i>R</i> ₁ ^[a] [<i>I</i> > 2σ(<i>I</i>)]	0.0524	0.0508
<i>wR</i> ₂ ^[b] [<i>I</i> > 2σ(<i>I</i>)]	0.1227	<i>wR</i> ₂ = 0.1250

[a] $R_1 = \Sigma||F_o| - |F_c||/\Sigma|F_o|$. [b] $wR_2 = \{\Sigma[w(F_o^2 - F_c^2)^2]/\Sigma[w(F_o^2)]\}^{1/2}$.

Acknowledgments

This work was supported by the National Natural Science Foundation of China (No. 20771083, No. 20631030 and No. 20771081) and National Basic Research Program of China, 973 Program, 2007CB815305.

- [1] a) O. Kahn, *Molecular Magnetism*, VCH, New York, **1993**; b) D. Gatteschi, O. Kahn, J. S. Miller, F. Palacio, *Molecular Magnetic Materials*, NATO ASI Series, Kluwer, Dordrecht, The Netherlands, **1991**; c) E. Coronado, P. Delhaès, D. Gatteschi, J. S. Miller, *Molecular Magnetism: From Molecular Assemblies to the Devices*, Kluwer, Dordrecht, The Netherlands, **1996**; d) D. Gatteschi, A. Caneschi, R. Sessoli, A. Cornia, *Chem. Soc. Rev.* **1996**, 101–109; e) D. L. Popescu, A. Chanda, M. Stadler, F. T. Oliveira, A. D. Ryabov, E. Münck, E. L. Bominaar, T. J. Collins, *Coord. Chem. Rev.* **2008**, 252, 2050–2071; f) W. Lewan-

- dowski, M. Kalinowska, H. Lewandowska, *J. Inorg. Biochem.* **2005**, *99*, 1407–1423; g) G. Mezei, C. M. Zaleski, V. L. Pecoraro, *Chem. Rev.* **2007**, *107*, 4933–5003.
- [2] a) O. Kahn, *Adv. Inorg. Chem.* **1996**, *43*, 179; b) O. Kahn, J. Galy, Y. Journaux, J. Jaud, I. Morgestern-Badarau, *J. Am. Chem. Soc.* **1982**, *104*, 2165–2176; c) V. Baron, B. Gillon, O. Plantevin, A. Cousson, C. Mathonière, O. Kahn, A. Grand, L. Ohrstrom, B. Delley, *J. Am. Chem. Soc.* **1996**, *118*, 11822–11830; d) O. Sato, T. Iyoda, A. Fujishima, K. Hashimoto, *Science* **1996**, *272*, 704–705; e) P. Chaudhuri, *Coord. Chem. Rev.* **2003**, *243*, 143–190; f) S. Tanase, J. Reedijk, *Coord. Chem. Rev.* **2006**, *250*, 2501–2510.
- [3] a) O. Kahn, Y. Pei, M. Verdager, J. P. Renard, J. Sletten, *J. Am. Chem. Soc.* **1988**, *110*, 782–787; b) K. Nakatani, J. Y. Carriat, Y. Journaux, O. Kahn, F. Lloret, J. P. Renard, Y. Pei, J. Sletten, M. Verdager, *J. Am. Chem. Soc.* **1989**, *111*, 5739–5748; c) E. Pardo, R. Ruiz-García, F. Lloret, J. Faus, M. Julve, Y. Journaux, M. A. Novak, F. S. Delgado, C. Ruiz-Pérez, *Chem. Eur. J.* **2007**, *13*, 2054–2066; d) A. Neels, H. Stoeckli-Evans, S. A. Chavan, J. V. Yakhmi, *Inorg. Chim. Acta* **2001**, *326*, 106–110; e) O. Cadot, M. G. F. Vaz, H. O. Stumpf, C. Mathonière, O. Kahn, *Synth. Met.* **2001**, *122*, 559–567; f) E. Pardo, R. Ruiz-García, J. Cano, X. Ottenwaelder, R. Lescouëzec, Y. Journaux, F. Lloret, M. Julve, *Dalton Trans.* **2008**, 2780–2805; g) O. Kahn, *Acc. Chem. Res.* **2000**, *33*, 647–657.
- [4] a) M. Julve, M. Verdager, G. DeMunno, J. A. Real, G. Bruno, *Inorg. Chem.* **1993**, *32*, 795–802; b) J. M. Clemente-Juan, C. Mackiewicz, M. Verelst, F. Dahan, A. Bousseksou, Y. Sanakis, J. P. Tuchagues, *Inorg. Chem.* **2002**, *41*, 1478–1491; c) P. Talukder, A. Datta, S. Mitra, G. Rosair, M. Salah, E. Fallah, J. Ribas, *Dalton Trans.* **2004**, 4161–4167; d) A. K. Boudalis, J. M. Clemente-Juan, F. Dahan, J. P. Tuchagues, *Inorg. Chem.* **2004**, *43*, 1574–1586.
- [5] a) M. Montfort, J. Ribas, X. Solans, *Inorg. Chem.* **1994**, *33*, 4271–4276; b) R. Vicente, A. Escuer, J. Ribas, X. Solans, *J. Chem. Soc., Dalton Trans.* **1994**, 259–262; c) K.-L. Zhang, W. Chen, Y. Xu, Z. Wang, Z. J. Zhong, X.-Z. You, *Polyhedron* **2001**, *20*, 2033; d) F. A. Mautner, R. Vicente, S. S. Massoud, *Polyhedron* **2006**, *25*, 1673–1680; e) M. Kabešová, R. Boča, M. Melnik, D. Valigura, M. Dunaj-Jurko, *Coord. Chem. Rev.* **1995**, *140*, 115–135; f) F. Noreen, T. Rüffer, H. Lang, A. A. Isab, S. Ahmad, *J. Chem. Crystallogr.* **2008**, *38*, 765–768; g) S. Ferlay, G. Francesse, H. W. Schmalte, S. Decurtins, *Inorg. Chim. Acta* **1999**, *286*, 108–113; h) J. Mroziński, J. Klak, R. Kruszyński, *Polyhedron* **2008**, *27*, 1401–1407.
- [6] a) A. Beheshti, W. Clegg, R. Hyvadi, H. Fereshteh Hekmat, *Polyhedron* **2002**, *21*, 1547–1552; b) R. Vicente, A. Escuer, J. Ribas, X. Solans, M. Font-Bardía, *Inorg. Chem.* **1993**, *32*, 6117–6118.
- [7] a) A. Das, G. M. Rosair, M. S. El Fallah, J. Ribas, S. Mitra, *Inorg. Chem.* **2006**, *45*, 3301–3306; b) S. Demeshko, G. Leibel, S. Dechert, F. Meyer, *Dalton Trans.* **2006**, 3458–3465; c) Y. Z. Zhang, W. Wernsdorfer, F. Pan, Z. M. Wang, S. Gao, *Chem. Commun.* **2006**, 3302–3304; d) A. K. Ghosh, D. Ghoshal, E. Zangrando, J. Ribas, N. Ray Chaudhuri, *Inorg. Chem.* **2005**, *44*, 1786–1793; e) Y. Song, C. Massera, O. Roubeau, P. Games, A. M. Lanfredi, J. Reedijk, *Inorg. Chem.* **2004**, *43*, 6842–6847; f) S. Koner, S. Saha, T. Mallah, K. Okamoto, *Inorg. Chem.* **2004**, *43*, 840–842; g) J. Ribas, A. Escuer, M. Monfort, R. Vicente, R. Cortés, L. Lezama, T. Rojo, *Coord. Chem. Rev.* **1999**, *193*–195, 1027–1068; h) L. Lecren, O. Roubeau, C. Colun, Y. G. Li, X. F. L. Goff, W. Wernsdorfer, H. Miyasaka, R. Clérac, *J. Am. Chem. Soc.* **2005**, *127*, 17353–17363.
- [8] a) H. Miyasaka, K. Nakata, L. Lecren, C. Coulon, Y. Nakazawa, T. Fujisaki, K. Sugiura, M. Yamashita, R. Clérac, *J. Am. Chem. Soc.* **2006**, *128*, 3770–3783; b) J. L. Manson, J. Gu, J. A. Schlueter, H. H. Wang, *Inorg. Chem.* **2003**, *42*, 3950–3955; c) J. L. Manson, A. M. Arif, C. D. Incarvito, L. M. Liable-Sands, A. L. Rheingold, J. S. Miller, *J. Solid State Chem.* **1999**, *145*, 369–378.
- [9] a) O. V. Nesterova, S. R. Petrusenko, V. N. Kokozay, B. W. Skelton, J. Jezierska, W. Linert, A. Ozarowski, *Dalton Trans.* **2008**, 1431–1436; b) L.-N. Zhu, N. Xu, W. Zhang, L.-Z. Liao, K. Yoshimura, K. Mibu, Z.-H. Jiang, S.-P. Yan, P. Cheng, *Inorg. Chem.* **2007**, *46*, 1297–1304; c) A. D. Jana, S. C. Manna, G. M. Rosair, M. G. B. Drew, G. Mostafa, N. R. Chaudhuri, *Cryst. Growth Des.* **2007**, *7*, 1365–1372; d) S. B. Wang, G. M. Yang, R. F. Li, Y. F. Wang, D. Z. Liao, *Eur. J. Inorg. Chem.* **2004**, 4907–4913; e) C. S. Li, L. Xue, Y. X. Che, F. Luo, J. M. Zheng, T. C. W. Mak, *Inorg. Chim. Acta* **2007**, *360*, 3569–3574; f) I. Ondrejková, S. Galkova, J. Mroziński, J. Klak, T. Lis, Z. Olejnik, *Inorg. Chim. Acta* **2008**, *361*, 2483–2490; g) Y. F. Yue, C. J. Fang, E. Q. Gao, C. He, S. Q. Bai, S. Xu, C. H. Yan, *J. Mol. Struct.* **2008**, *875*, 80–85; h) F. A. Mautner, R. Vicente, S. S. Massoud, *Polyhedron* **2006**, *25*, 1673–1680; i) D. J. Darzensbourg, E. B. Frantz, *Inorg. Chem.* **2008**, *47*, 1297–1304.
- [10] G. Francesse, S. Ferlay, H. W. Schmalte, S. Decurtins, *New J. Chem.* **1999**, 267–269.
- [11] a) S. Ferlay, T. Mallah, J. Vaissermann, F. Bartolome, P. Veillet, M. Verdager, *Chem. Commun.* **1996**, 481; b) J. Zou, X. Hu, Ch. Duan, Z. Xu, X. You, *Transition Met. Chem.* **1998**, *23*, 477–480; c) E. Colacio, J. M. Dominguez-Vera, M. Ghazi, R. Kivekas, M. Klinga, J. M. Moreno, *Chem. Commun.* **1998**, *10*, 1071–1072; d) E. Colacio, J. M. Dominguez-Vera, M. Ghazi, R. Kivekas, F. Lloret, J. M. Moreno, H. Stoeckli-Evans, *Chem. Commun.* **1999**, *11*, 987–988; e) H. Z. Kou, S. Gao, W. M. Bu, D. Z. Liao, B. Q. Ma, Z. H. Jiang, S. P. Yan, Y. G. Fan, G. L. Wang, *J. Chem. Soc., Dalton Trans.* **1999**, 2477–2480; f) H. Z. Kou, S. Gao, B. Q. Ma, D. Z. Liao, *Chem. Commun.* **2000**, 713–714; g) E. Colacio, J. M. Dominguez-Vera, M. Ghazi, R. Kivekas, J. M. Moreno, A. Pajunen, *J. Chem. Soc., Dalton Trans.* **2000**, 505–509.
- [12] a) H. Ojima, K. Nonoyama, *Coord. Chem. Rev.* **1988**, *92*, 85; b) R. Ruiz, J. Faus, F. Lloret, M. Julve, Y. Journaux, *Coord. Chem. Rev.* **1999**, *193*, 1069–1117.
- [13] F. Lloret, Y. Journaux, M. Julve, *Inorg. Chem.* **1990**, *29*, 3967–3972.
- [14] a) H. Okawa, Y. Kawahara, M. Masahiro, S. Kida, *Bull. Chem. Soc. Jpn.* **1980**, *53*, 549; b) L. Banci, A. Bencini, C. Benelli, D. Getteschi, *Inorg. Chem.* **1981**, *20*, 1399–1402; c) Y. Journaux, J. Sletten, O. Kahn, *Inorg. Chem.* **1985**, *24*, 4063–4069; d) Y. Journaux, J. Sletten, O. Kahn, *Inorg. Chem.* **1986**, *25*, 437–439; e) F. Lloret, M. Julve, J. Faus, R. Ruiz, I. Castro, M. Mollar, M. Philoche-Levisalles, *Inorg. Chem.* **1992**, *31*, 784–791; f) A. Escuer, R. Vicente, J. Ribas, R. Costa, X. Solans, *Inorg. Chem.* **1992**, *31*, 2627–2633; g) F. Lloret, M. Julve, R. Ruiz, Y. Journaux, K. Nakatani, O. Kahn, J. Sletten, *Inorg. Chem.* **1993**, *32*, 27–31; h) C. Mathoniere, O. Kahn, J. C. Daran, H. Hilbig, F. H. Kohler, *Inorg. Chem.* **1993**, *32*, 4057–4062.
- [15] a) Z. Y. Zhang, D. Z. Liao, Z. H. Jiang, S. Q. Hao, X. K. Yao, H. G. Wang, G. L. Wang, *Inorg. Chim. Acta* **1990**, *173*, 201; b) J. A. Real, R. Ruiz, J. Faus, M. Julve, Y. Journaux, M. Phioche-Levisalles, C. Bois, *J. Chem. Soc., Dalton Trans.* **1994**, 3769–3773; c) J. L. Sanz, R. Ruiz, A. Gleizes, F. Lloret, J. Faus, M. Julve, J. J. Borrás-Almenar, Y. Journaux, *Inorg. Chem.* **1996**, *35*, 7384–7393; d) J. Larionova, S. A. Chavan, J. V. Yakhmi, A. G. Frøystein, J. Sletten, C. Sourisseau, O. Kahn, *Inorg. Chem.* **1997**, *36*, 6374–6381; e) Z. N. Chen, H. X. Zhang, K. B. Yu, B. S. Kang, H. Cai, C. Y. Su, T. W. Wang, Z. L. Lu, *Inorg. Chem.* **1998**, *37*, 4475–4781; f) J. Ribas, C. Diaz, R. Costa, J. Tercero, X. Solans, M. Font-Bardía, H. Stoeckli-Evans, *Inorg. Chem.* **1998**, *37*, 233–239.
- [16] a) J. M. Dominguez-Vera, J. M. Moreno, N. Galvez, J. Suarez-Varela, E. Colacio, R. Kivekas, M. Klinga, *Inorg. Chim. Acta* **1998**, *281*, 95–100; b) C. Diaz, J. Ribas, R. Costa, J. Tercero, M. S. El Fallah, X. Solans, M. Font-Bardía, *Eur. J. Inorg. Chem.* **2000**, 675–681; c) I. Castro, M. L. Calatayud, J. Sletten, M. Julve, F. C. Llort, *R. Acad. Sci. Ser. IIC: Chim.* **2001**, 235–243; d) N. Fukita, M. Ohba, T. Shiga, H. Ohkawa, Y. Ajiro, *J. Chem. Soc., Dalton Trans.* **2001**, 64–70; e) S. Q. Zang, R. J.

- Tao, Q. L. Wang, N. H. Hu, Y. X. Cheng, J. Y. Niu, D. Z. Liao, *Inorg. Chem.* **2003**, 42, 761–766.
- [17] A. W. Addison, T. N. Rao, J. Reedijk, J. Vanrijn, G. C. Verschoor, *J. Chem. Soc., Dalton Trans.* **1984**, 1349–1356.
- [18] K. Nakamoto, *Infrared and Raman Spectra of Inorganic and Coordination Compounds, Part B*, 5th ed., John Wiley, New York, **1997**.
- [19] B. J. Hathaway, *Struct. Bonding (Berlin)* **1973**, 14, 49.
- [20] a) J. K. Tang, L. Y. Wang, L. Zhang, E. Q. Gao, D. Z. Liao, Z. H. Jiang, S. P. Yan, P. Cheng, *J. Chem. Soc., Dalton Trans.* **2002**, 1607–1612; b) J. K. Tang, S. F. Si, L. Y. Wang, D. Z. Liao, Z. H. Jiang, S. P. Yan, P. Cheng, X. Liu, *Inorg. Chim. Acta* **2003**, 343, 288–294; c) J. K. Tang, Q. L. Wang, E. Q. Gao, J. T. Chen, D. Z. Liao, Z. H. Jiang, S. P. Yan, P. Cheng, *Helv. Chim. Acta* **2002**, 85, 175–182; d) Z. L. Liu, D. Q. Zhang, J. L. Luo, Z. H. Jiang, D. Z. Liao, D. B. Zhu, *J. Coord. Chem.* **2004**, 57, 647–655; e) V. A. White, R. D. L. Johnstone, K. L. McCall, N. J. Long, A. M. Z. Slawin, N. Robertson, *Dalton Trans.* **2007**, 2942–2948.
- [21] a) E. Q. Gao, J. K. Tang, D. Z. Liao, Z. H. Jiang, S. P. Yan, G. L. Wang, *Helv. Chim. Acta* **2001**, 84, 908–917; b) N. Fukita, M. Ohba, T. Shiga, H. Okawa, Y. Ajiro, *J. Chem. Soc., Dalton Trans.* **2001**, 54–70; c) E. Q. Gao, D. Z. Liao, Z. H. Jiang, S. P. Yan, *Polyhedron* **2001**, 20, 923–927; d) J. K. Tang, S. F. Si, E. Q. Gao, D. Z. Liao, Z. H. Jiang, S. P. Yan, *Inorg. Chim. Acta* **2002**, 332, 146–152; e) R. J. Tao, S. Q. Zang, Y. X. Cheng, Q. L. Wang, N. H. Hu, J. Y. Niu, D. Z. Liao, *Polyhedron* **2003**, 22, 2911–2916.
- [22] F. Lioret, M. Julve, J. Cano, R. Ruiz-García, E. Pardo, *Inorg. Chim. Acta* **2008**, 361, 3432–3445.
- [23] O. Kahn, P. Tola, H. Coudanne, *Chem. Phys.* **1979**, 42, 355.
- [24] D. S. C. Black, H. Corrie, *Inorg. Nucl. Chem. Lett.* **1976**, 12, 65–71.
- [25] P. W. Selwood, *Magnetochemistry*, Interscience, New York, **1956**, p. 78.
- [26] G. M. Sheldrick, *SHELXS-97, SHELXL-97, Software for Crystal Structure, Analysis*, Siemens Analytical X-ray Instruments. Inc., Madison, WI, **1997**.

Received: December 20, 2008
Published Online: May 26, 2009